

Energy Dispersion Relations for Holes in Silicon Quantum Wells and Quantum Wires

V. V. Mitin, N.Z. Vagidov, M. Luisier¹, and Gerhard Klimeck²

University at Buffalo, SUNY, 332D Bonner Hall, Buffalo, NY 14260, USA

¹Integrated Systems Laboratory, ETH Zurich, 8092 Zurich, Switzerland

²Network for Computational Nanotechnology, Purdue University, West Lafayette, IN 47907, USA
e-mail: vmitin@buffalo.edu

INTRODUCTION

Energy dispersion relations, $E(\mathbf{k})$, for holes in low-dimensional structures of silicon are substantially richer than those for electrons. In particular, there are extensive regions with negative effective masses (NEM) in $E(\mathbf{k})$, i.e. regions where second derivative of E upon \mathbf{k} changes its sign. Here an empirical $sp^3d^5s^*$ tight-binding model which includes interaction of each atom with its nearest neighbors and takes into account ten of its atomic orbitals: s - and excited s^* -orbitals, three p -, and five d -orbitals is used. The inclusion of higher d -orbitals and spin-orbital coupling dramatically improves the precision of the calculated electron and hole dispersion relations [1]. Quantum wells (QW) and quantum wires (QWR) are considered.

RESULTS AND DISCUSSION

$E(\mathbf{k}_{2D})$ for QWs for different orientations of the two-dimensional vector \mathbf{k}_{2D} in the plane of the well and for different QW growth directions \mathbf{n} are computed. The results obtained for a wide range of well thickness show that the dispersion relations strongly depend on the direction of \mathbf{k}_{2D} in the plane of the QW as well as on direction of \mathbf{n} . In particular, for a $\mathbf{k}_{2D} \parallel [100]$ the dispersion relations have small values of NEM. For $\mathbf{k}_{2D} \parallel [110]$ the NEM sections are well pronounced as it is shown in Fig. 1. Kramers' degeneracy is lifted for most of combinations of considered \mathbf{k}_{2D} and \mathbf{n} .

For QWRs grown in $[100]$ direction (x -axis) and rectangular cross section (axes y and z are in $[010]$ and $[001]$ directions, respectively) the quantization energy is substantially larger than for QWRs of other growth directions, but the dispersion curves are almost flat with large effective masses and with

almost no regions with NEM as shown in Fig. 2(a). For wires grown in $[110]$ direction (x -axis) and rectangular cross section (axes y and z are in $[-110]$ and $[001]$ directions, respectively) the dispersion curves have well pronounced regions with NEM. The Kramers' degeneracy for $\mathbf{k}_{1D} \parallel [100]$ is not lifted, whereas for $\mathbf{k}_{1D} \parallel [110]$ a lift of degeneracy is well pronounced.

Finally, Fig. 3 presents a discussion on the analytical analysis of obtaining $E(\mathbf{k})$ of a QWR using $E(\mathbf{k})$ of the QW. This approach provides insights into the general behavior of the expected $E(\mathbf{k})$ in QWRs before the QWR simulations are performed.

CONCLUSION

QWs as well as QWRs can exhibit well pronounced regions of NEM which may find significant applications in active components of circuits. The critical design parameters, such as splitting between the lowest and upper subbands, Δ , as well as the magnitude of the wave vector, k_c , when the NEM occurs, and the energy interval with NEM, are sensitive to the directions of confinement as well as to the direction of \mathbf{k} .

ACKNOWLEDGEMENT

This work was supported by Petroleum Research Fund Grant No. 41317-AC10, NSF Grant No. EEC-0228390, and the Indiana 21st Century Fund.

REFERENCES

- [1] A. Rahman, G. Klimeck, M. Lundstrom, N. Vagidov, and T.B. Boykin, *Jap. J. of Applied Physics* **44**, 2187 (2005).
- [2] The $sp^3d^5s^*$ model includes spin and spin-orbit coupling explicitly. These simulations do not include any external magnetic field that would provide spin selection. The splitting of the states is purely due to symmetry breaking and the two split states are a mixture of up and down spins.

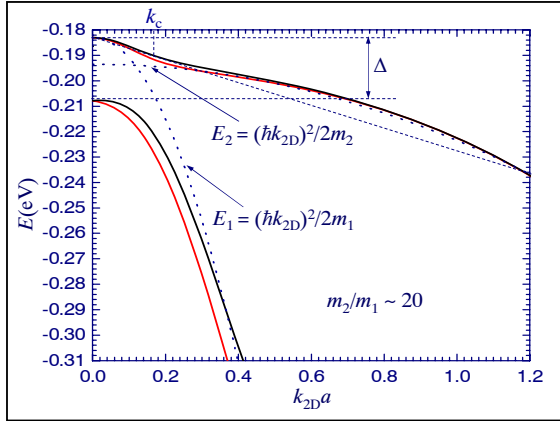


Fig. 1. Dispersion relations $E(\mathbf{k}_{2D})$ for holes in a silicon QW for $\mathbf{k}_{2D} \parallel [110]$. The thickness of QW is 1.63 nm. Δ is the energy gap between the lowest and next hole subbands, k_c is an inflection point where NEM region starts, and a is the Si lattice constant equal to 5.43 Å. Black and red curves relate to two different spins [2].

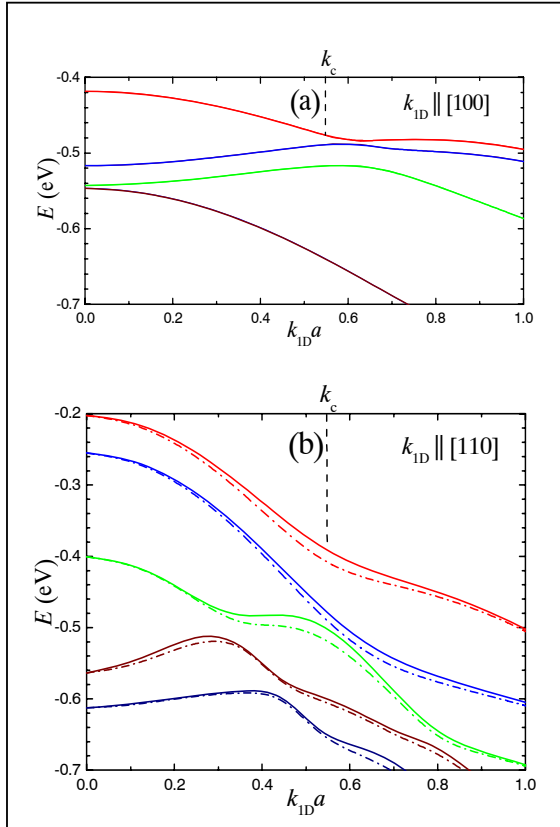


Fig. 2. Dispersion relations $E(\mathbf{k}_{1D})$ for holes in a silicon QW: (a) in the direction [100] with cross section 1.63 nm in direction [001] and 1.63 nm in direction [010]; (b) in the direction [110] with cross section 1.63 nm in direction [001] and 1.73 nm in direction [-110]. Solid and dash-dotted curves correspond to different spins [2].

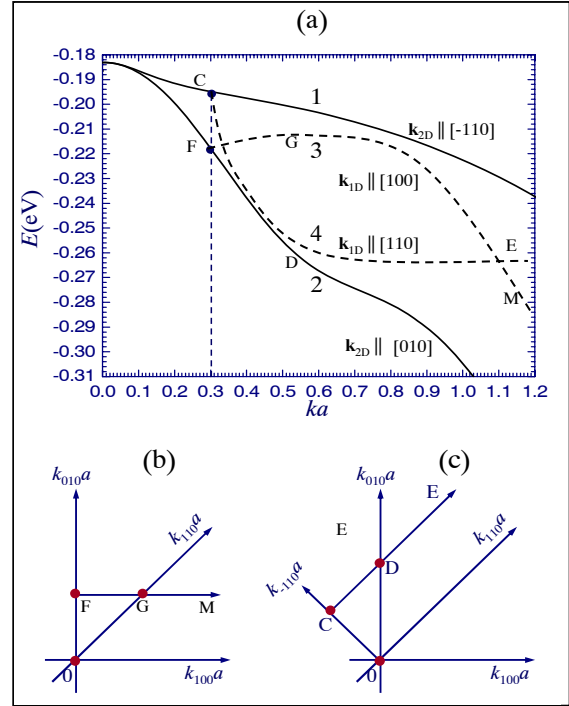


Fig. 3. (a) Solid curves show calculated $E(\mathbf{k}_{2D})$ for a QW in a plane (001) and two directions of the two-dimensional vector, \mathbf{k}_{2D} , in the plane of the well: $\mathbf{k}_{2D} \parallel [-110]$ (curve 1) and $\mathbf{k}_{2D} \parallel [010]$ (curve 2). QW thickness is 1.63 nm.

Qualitative behavior of the dispersion relations in QWRs are shown by dashed curves and they are obtained using the following procedure. The qualitative curves, $E(\mathbf{k}_{1D})$, for a QWR can be presented as slices of the dispersion relations of thin films, $E(\mathbf{k}_{2D})$, assuming that $\mathbf{k}_{2D} = \mathbf{k}_{1D} + \mathbf{k}_Q$ where $k_Q \approx \pi/d$ corresponds to the quantized wave vector in the plane of the film perpendicular to the direction \mathbf{k}_{1D} and d is the wire thickness in that direction. For demonstration purposes we have chosen $ka = 0.3$.

For curve 3 $\mathbf{k}_{1D} \parallel [100]$. As k_{1D} increases, the vector $\mathbf{k}_{2D} = \mathbf{k}_{1D} + \mathbf{k}_Q$ deviates from the direction [010] (point F in Figs. 3(a) and 3(b)) towards the direction [110] and then towards [100]. At $k_{1D} = k_Q$ vector \mathbf{k}_{2D} is parallel to [110] and this is why $E(\mathbf{k}_{1D})$ tends first to point G (or curve 1) and with the further increase of k_{1D} it tends to curve 2 as k_{1D} becomes substantially larger than k_Q (point M on Figs. 3(a) and 3(b)).

For curve 4 $\mathbf{k}_{1D} \parallel [110]$. As k_{1D} increases, the vector $\mathbf{k}_{2D} = \mathbf{k}_{1D} + \mathbf{k}_Q$ deviates from the direction [-110] (point C in Figs. 3(a) and 3(c)) towards the direction [010] and then towards [110]. At $k_{1D} = k_Q$ vector \mathbf{k}_{2D} is effectively parallel to [010] and this is why $E(\mathbf{k}_{1D})$ tends first to point D (or curve 2) and with the further increase of k_{1D} it tends to curve 1 as k_{1D} becomes substantially larger than k_Q (point E on Figs. 3(a) and 3(c)).

We present this method of slicing because it allows one to get qualitative behavior of dispersion curves in QWRs and to identify the favorable directions of QWRs for more detailed calculations of $E(\mathbf{k})$ (as presented in Fig.2) instead of running the time-consuming detailed QWR numerical calculations for all possible directions. Analogous analysis can be used to obtain qualitative $E(\mathbf{k})$ in QWs by slicing $E(\mathbf{k})$ of bulk silicon.